Engineering Structures 195 (2019) 263–273

Contents lists available at ScienceDirect

Engineering Structures

journal homepage: www.elsevier.com/locate/engstruct

Analysis of combined action of seismic loads and alkali-silica reaction in concrete dams considering the key chemical-physical-mechanical factors and fluid-structure interaction

Mohammad S. Pourbehi*, Gideon P.A.G. van Zijl, J.A.vB. Strasheim

Division for Structural Engineering and Civil Engineering Informatics, Stellenbosch University, South Africa

ARTICLE INFO

Keywords:
Alkali silica reaction
Concrete dams
Seismic analysis
Fluid structure interaction

ABSTRACT

This paper presents the results of the numerical analysis of concrete dam structures which are affected by Alkali Silica Reaction (ASR) and subjected to seismic load. In this research a Chemo-Thermo-Mechanical ASR Finite Element numerical code is developed to model and analyse this phenomenon in concrete dams. It considers the effects of variables such as temperature, non-uniform time-dependent material degradation and 3D stress confinement on ASR evolution. The model is validated by modelling the mechanical response of the Fontana gravity dam and comparing the results with the actual data on macro crack appearance and crest displacement. While the structural behaviour of ASR affected structures under monotonic and quasi-static loading has been extensively investigated over the last decades, limited research has addressed the effect of dynamic loads on structures affected by ASR. The combined effect of old and new cracks under dynamic excitation may cause dam failure. The numerical simulations are used to assess and predict the dynamic stability of the Koyna dam considering fluid-structure interaction and are also used to investigate the evolution of damage associated with inception and development of macro cracks in the dam structure due to the combined effect of the synthetic ASR and realistic seismic loading on the dam. The results show that this combined action can significantly change the dynamic behaviour of typical concrete dams due to concrete material degradation and crack development.

1. Introduction

Dams are important infrastructure components and an asset for any country. Past earthquakes have highlighted their vulnerability to damage and even failure which can have major socio-economic consequences, losses and other cascading effects on e.g. water supply, power generation and irrigation. Hence, considerable efforts have been devoted to evaluate the safety of the aged dams and in some cases to pursue a suitable remedial action and rehabilitation strategy. Alkali Silica Reaction (ASR), a deleterious chemical reaction between siliceous aggregate and cement paste in concrete causes long term swelling and deterioration of concrete structures such as dams. The hydrophilic ASR gel expands in the presence of water, and initially fills the pores and micro cracks in the interfacial transition zone (ITZ) [1,2]. If reactive silica is not available at the aggregate surface, but contained within the aggregate particle, it takes time for the pore solution to diffuse into the aggregate and reach the reactive silica components. In such cases, the reaction proceeds more slowly and the gel forms within the aggregates. Thus, according to the mineralogy of aggregates, expansive gel may occur at the interior of the aggregate, or within the reaction rim at the cement paste-aggregate interface, leading to the distinction of late-expansive and early-expansive aggregates [3]. Further expansion induces a build-up of internal pressure, which is the main mechanism of initiation and propagation of cracks and degradation of elastic properties. Three requirements for onset and development of ASR are: (i) The presence of reactive silica in critical proportion. (ii) Sufficiently high alkali hydroxide concentration to trigger and sustain the reaction. (iii) Available water to initiate the reaction and drive the swelling of the gel. Several important factors govern the ASR reaction kinetics, of which moisture levels in and the temperature of the concrete are the most important [4–6]. ASR is thermo-activated; that is, the higher the temperature, the faster it occurs [2]. Numerical modelling should capture the impact of humidity, temperature distribution, kinetics of the reaction and 3D confining stresses as the most prominent factors influencing ASR.

ASR driven material expansion may be strongly coupled with internal damage [7]. Whether degraded structures can still resist natural events such as seismic excitation is a concern. While the mechanical

* Corresponding author.
E-mail address: mpourbehi@sun.ac.za (M.S. Pourbehi).

https://doi.org/10.1016/j.engstruct.2019.05.087
Received 12 October 2018; Received in revised form 17 April 2019; Accepted 28 May 2019
Available online 10 June 2019
0141-0296/

performance of ASR affected structures under monotonic and quasi-static loading has been extensively investigated over the last decades, limited research has addressed dynamic loading. The combined action of old and new cracks under dynamic excitation may cause dam failure. Considering predicted interaction between ASR and seismic loads, remedial measures can be adopted at the right time to safeguard the dam in the event of an earthquake. Fluid-Foundation-Structure Interaction (FFSI) also has received much attention in Finite Element Analysis (FEA) of dams. They include the effects of hydrodynamic pressure on the dam-water interface, and assumed boundary conditions on the fluid domain, such as far-field non-reflective and the admittance boundary condition for modelling the sediments in the reservoir bed [8,9].

In general, numerical models for modelling ASR and its effects fall into three categories: (i) macrostructural models concerned with the analysis of structures affected by the reaction [2,10,11,12]; (ii) microstructural models which link the chemical reaction to its impact at the material level [1,13]; (iii) mesoscopic models [14,15] that consider the multi-phases of the aggregate, cement paste, void and ASR gel, whereby material anisotropy is explicitly represented. Esposito and Hendriks [16] present a comprehensive review of modelling approaches, investigating how the level of approach may enable the chemistry of ASR to be captured accurately, but not necessarily accurately capture the impact on the structural level. They identify the research need towards a modelling approach which can downscale to ion diffusion-reaction processes to accurately capture reaction products, but also upscale to structural level. In the study presented here, a macroscopic approach is followed, considering chemo-thermo-mechanics which incorporates the influence of temperature on the rate of ASR expansion, and captures non-uniform, time-dependent material degradation and 3D stress confinement effects on ASR evolution. The kinematic The model is validated by modelling the mechanical response of the Fontana gravity dam and comparing the results with the actual data on macro crack appearance and crest displacement reported by Ingraffea [17] and other numerical models available in literature [18].

Currently, no practical methods to curb or arrest the swelling chemical reaction in existing concrete dams due to ASR have been developed. A numerical model that can predict the long term behaviour of and the potential damage to a structure subject to ASR can provide engineers with a tool to properly plan the rehabilitation and remedial action. The majority of research has ignored the long-term effects of material degradation that may change the engineering properties of the dam material during the service life of the dam [8,9]. Material degradation may significantly affect the dynamic behaviour of the dam, and it is necessary to estimate the seismic safety of the dams suffering from the ASR considering the time-dependent material deterioration. Research has been performed on aged concrete dams assuming a uniform material time dependent degradation index along the dam body, due to physical and chemical attacks such as freeze-thaw cycles, fatigue and expansive chemical reactions [19]. However, a uniform material deterioration index for the dam may be a conservative assumption and can result in the inaccurate determination of structural dynamic response and behaviour of the damaged structure.

Finally, the model is used to analyse and predict the dynamic behaviour of the Koyna dam, damaged by an earthquake [9,20]. The combined ASR and seismic action is investigated and comparisons are made through a comprehensive study of the damage extent and crest displacement. The seismic response of the deteriorated dam is subsequently analysed based on the state of the structure at the end of the long-term ASR analysis. The results show that combined action can significantly change the dynamic behaviour of concrete dams.

2. Chemo-thermo-mechanical modelling of ASR

A chemo-thermo-mechanical finite element (FE) model is developed to model and analyse the behaviour of dam structures under ASR induced expansion and resulting material degradation and structural deterioration. Temperature fields, kinetics of the reaction and confining stresses are incorporated. The finite element model simulates the temperature spatial and temporal fields in the structure and how they influence the kinetics of the chemical reaction to predict long-term effects of ASR in concrete structures. For simplicity one-way coupling only is considered, i.e. the temperatures are not dependent on the subsequent chemical and mechanical response. FFSI with appropriate boundary conditions in the fluid medium and interactive surfaces is considered to model a realistic hydrodynamic pressure induced by reservoir waves induced by seismic waves.

2.1. Mechanical modelling strategy

The Concrete Damage Plastic (CDP) model by Lee and Fenves [21] is used to capture concrete mechanical behaviour. The model is implemented in Abaqus [22] and a user subroutine is developed to establish a link between strain rate from ASR and damage plastic modelling. In summary, in the chemo-thermo-mechanical model, the directional Cauchy stress rate is given by:

$$\dot{\sigma} = (1-\phi)\dot{\sigma}_{eff} = (1-\phi)\boldsymbol{D}_0^{\boldsymbol{e}}(\dot{\boldsymbol{\varepsilon}} - \dot{\boldsymbol{\varepsilon}}^{\boldsymbol{pl}} - \dot{\boldsymbol{\varepsilon}}^{\boldsymbol{th}} - \dot{\boldsymbol{\varepsilon}}^{\boldsymbol{asr}}) \tag{1}$$

where $\boldsymbol{D}_0^{\boldsymbol{e}}$ is the initial (undamaged) constitutive material stiffness tensor, $\dot{\boldsymbol{\varepsilon}}$ denotes the total strain rate vector, $\dot{\boldsymbol{\varepsilon}}^{\boldsymbol{pl}}$ is the plastic strain rate vector, $\dot{\boldsymbol{\varepsilon}}^{\boldsymbol{th}}$ is the thermal strain rate vector and $\dot{\boldsymbol{\varepsilon}}^{\boldsymbol{asr}}$ is the ASR-induced strain rate vector. The thermal strain is governed by the thermal coefficient α and the temperature increment. The damage index ϕ of the ASR affected concrete consists of the mechanical part (d_m) caused by mechanical loads and the chemical part (d_{asr}) induced by ASR, and thus the damage index is defined as:

$$\phi = 1 - (1-d_{asr})(1-\mathrm{d}_m) \tag{2}$$

The yield function represents the surface in effective stress space, which determines the states of failure or damage to account for different evolution of strength under monotonic or cyclic tensile and compressive loads, is used as [20]:

$$F(\bar{\boldsymbol{\sigma}}, \boldsymbol{\varepsilon}^{\boldsymbol{pl}}) = \frac{1}{1-\alpha}[\alpha I_1 + \sqrt{3J_2} + \hat{\beta}(\boldsymbol{\varepsilon}^{\boldsymbol{pl}})\langle\hat{\sigma}_{max}\rangle] - C_c(\boldsymbol{\varepsilon}^{\boldsymbol{pl}}) \leq 0 \tag{3}$$

where $\boldsymbol{\varepsilon}^{\boldsymbol{pl}}$ is the hardening variable; α and $\hat{\beta}$ are dimensionless material model constants; $I_1 = tr\sigma_{eff}$ and $J_2 = 1/2\boldsymbol{S}$: $\boldsymbol{S}$ with $\boldsymbol{S}$ the deviatoric part of the effective stress tensor $\bar{\sigma}$; $\hat{\sigma}_{max}$ is the maximum principal effective stress; C_c is the cohesion; and the Macaulay bracket has the definition of $\langle\chi\rangle = (\chi + |\chi|)/2$. The plastic strain rate is governed by non-associated plastic flow:

$$\dot{\boldsymbol{\varepsilon}}^{pl} = \dot{\lambda}\frac{\partial Q(\bar{\boldsymbol{\sigma}})}{\partial\bar{\boldsymbol{\sigma}}} \tag{4}$$

where λ is the non-negative plastic multiplier. The flow potential Q chosen for this model is the Drucker-Prager hyperbolic function [22]. The ultimate strain is given by

$$\varepsilon_u = \frac{2G_f}{f_t l_c} \tag{5}$$

with G_f is the fracture energy and f_t is the tensile strength. The length scale l_c is linked to the mesh size according to the crack band theory introduced by Bazant and Oh [23] to regularise fracture energy dissipation with respect to finite element size. Furthermore, the maximum element size is restricted to prevent snap-back within an element. For crack band theory to correctly regularize the computed cracking, cracks arising in a structure must be captured by a single row, column or diagonal strip of elements. It is acknowledged that full regularisation of both energy dissipation and crack orientation is not guaranteed by this approach, but refined regularization methods such as XFEM (Extended Finite Element Method) and rate-dependent material models fall outside the scope of this research.

Mechanical damage is defined by a linear softening law [24]:

$$d_m = \begin{cases} 0 & \kappa \leqslant \varepsilon_0 \\ 1 - \frac{f_t(\varepsilon_u - \kappa)}{E_0(\varepsilon_u - \varepsilon_0)(\kappa - \varepsilon^p)} & \varepsilon_0 < \kappa < \varepsilon_u \\ 1 & \kappa \geqslant \varepsilon_u \end{cases} \quad (6)$$

where $\varepsilon_0 = f_t/E_0$, E_0 is the initial elastic modulus, ε^p is uniaxial plastic strain and κ is the largest converged value of strains during the mechanical analysis.

2.2. ASR modelling strategy

The ASR strain rate variable $\dot{\varepsilon}^{asr}$ introduced in Eq. (1) is elaborated here. In this research it is assumed that the ASR induced strains are volumetric in nature in configurations without confining stresses. This assumption is considered by several researchers and experimental work demonstrated a reasonable agreement with numerical models considering volumetric strain [5,12]. In a recent experimental campaign by Liaduat et al. [25], a mechanical device was developed which is able to apply triaxial loads on ASR specimens for long periods of time for given specific environmental conditions. The results show that the ASR swelling is volumetric in the free stress state and transfers to the less compressed direction. A triaxial state of compressive stress equal to 9.7 MPa could totally suppressed the volumetric ASR expansions. In this research, an improved model by Saouma and Perotti [12] is used to define the ASR induced strains as:

$$\dot{\varepsilon}_i^{asr} = \Gamma_c(\sigma_v)\,\dot{\xi}\,[\tau_L(\theta, f(\sigma_v, f_c')), \tau_c(\theta)]\,\beta\, W_i(\sigma_v) \quad (7)$$

where Γ_c is the reduction function of 3D stress confinement, $\xi \in [0, 1]$ represents the extent of the ASR chemical reaction. Furthermore, $f_c^{'}$ is the cylinder compressive strength, β is the chemical dilation coefficient in the stress-free experiment and depends on the type of aggregates, mix proportion parameters, and the moisture content [2], and $W_i(\sigma_v)$ is a weighting function for distribution of the ASR strain in the principal stress directions depending on the volumetric stress σ_v. The parameters of Eq. (7) are elaborated next.

An extensive laboratory research programme by Larive [4] led to the development of the most promising reaction kinetics formulation. The reaction extent in the rate form is defined as:

$$\dot{\xi} = \frac{e^{t/\tau_c}(e^{\tau_l/\tau_c} + 1)}{\tau_c(e^{t/\tau_c} + e^{\tau_c/\tau_l})^2} \quad (8)$$

where τ_l and τ_c represent the latency and characteristic times respectively. The latency time and characteristic time are calculated based on the current temperature θ and the reference temperature $\bar{\theta}_0$, and isothermal laboratory tests have been conducted for their identification [4].

$$\tau_c(\theta) = \tau_c(\theta_0)\exp[U_c(1/\theta - 1/\bar{\theta}_0)], \quad (9a)$$

$$\tau_l(\theta, \sigma_v, f_c') = f(\sigma_v, f_c')\,\tau_l(\theta_0)\exp[U_L(1/\theta - 1/\bar{\theta}_0)] \quad (9b)$$

In addition, U_c and $U_L$are activation energy constants in Kelvin (K) and are defined as:

$$U_c = 5400 \pm 500\ \ K, \qquad U_L = 9400 \pm 500\ \ K. \quad (10)$$

Referring to Eq. (7), $f(\sigma_v, f_c^{'})$ is a retardation function that considers the increase in latency time due to the fact that micro cracks relevant to volumetric compression could likely absorb some gel which is produced during the chemical reaction. This mechanism could delay the ASR swelling initiation [12]:

$$f(\sigma_v, f_c') = \begin{cases} 1 & \sigma_v > 0 \\ 1 + \alpha\frac{\sigma_v}{3f_c'} & \sigma_v \leqslant 0 \end{cases} \quad (11)$$

where σ_v is the sum of compressive stresses in principal directions and α is 4/3 according to the Multon's tests [5].

ASR can be confined through different constraints. The forces from these constraints may be caused by the permanent loads such as gravity forces, or imposed loads such as hydrostatic loads in a reservoir. The forces may also arise due to ASR expansion restrained by boundary conditions. The effect of confinement stress on ASR expansion is considered through a reduction function which is applied to Eq. (7):

$$\Gamma_c = \begin{cases} 1 & \sigma_v \geqslant 0 \\ 1 - (\sigma_v/\bar{\sigma}_v)^2 & 0 \geqslant \sigma_v \geqslant \bar{\sigma}_v \\ 0 & \sigma_v \leqslant 0 \end{cases} \quad (12)$$

with $\bar{\sigma}_v$ a limit below which ASR is prevented, here assumed to be -9.7 MPa. Finally, $W_i(\sigma_v)$ is a weight function in each tensorial principal direction i.e. (i = 1, 2, 3). An effective technique is used to redistribute the ASR volumetric strain in each principal direction [26]. Practically it can determine the weight of ASR strain rate in each principal direction by introducing a decreasing function which links the weight of each direction to σ_v, volumetric stress equal to the sum of the stresses in principal direction.

The deterioration of the ASR-affected concrete is time-dependent, and the degradation of the elastic stiffness E and the tensile strength f_t are based on the ASR damage factor [11]:

$$E = E_0(1 - d_{asr}), \qquad f_t = f_{t0}(1 - d_{asr}) \quad (13)$$

E_0 and f_{t0} are the initial elastic modulus and tensile strength, respectively. During the ASR process, the swelling gels attack the concrete matrix and induces cracking of the aggregates and the surrounding cement paste. The damage leads to elastic modulus degradation. The ASR damage factor, d_{asr} may be linked to expansion strains from experimental results [27]:

$$d_{asr} = 1 - \frac{E}{E_0} = \frac{\max(\varepsilon_i^{asr})}{\max(\varepsilon_i^{asr}) + B} \quad (14)$$

where B has been calibrated to an approximate value of 0.3% [11].

2.3. Thermal analysis

Temperature history is a key factor driving the ASR in massive dams. Before performing the mechanical analysis, it is necessary to determine the temperature field in space and time. By assuming an initial condition for temperature θ_0 at time t_0 at each integration point in the dam, the FEA code is used to solve the transient thermal analysis:

$$\frac{\partial(\theta - \theta_0)}{\partial t} = D_\theta \frac{\partial^2(\theta - \theta_0)}{\partial x^2} \quad (15)$$

where $D_\theta = k/C$ denotes the thermal diffusivity (i.e., conductivity k divided by the volumetric heat capacity C). The results from thermal analysis are used in chemo-mechanical analysis through defining a predefined field temperature variation in space and time during the mechanical analysis. The user subroutine in the Abaqus FE code uses the temperature value at each integration point to compute the reaction extent and consequent ASR strains.

2.4. Fluid and structure interaction

The hydrodynamic pressure generated in the reservoir more than the hydrostatic pressure during motions of small amplitude is governed by the Helmholtz equation [28]:

$$\nabla^2 P = \frac{1}{C_0}\frac{\partial^2 P}{\partial t^2} \quad (16)$$

with P the hydrodynamic pressure, t the time and C_0 the acoustic wave speed in water. The FFSI system with boundary conditions for the upstream dam face, non-reflecting radiating boundary, admittance (sediment layer) and free surface boundary condition is shown in Fig. 1. The added-mass technique using the expression $M_{add} = \frac{7}{8}\rho_w\sqrt{h_w(h_w - y)}$ for $y \leqslant h_w$, is used to model the incompressible fluid assumption [8]. In this equation, ρ_w is the density of water, h_w is the water level in the

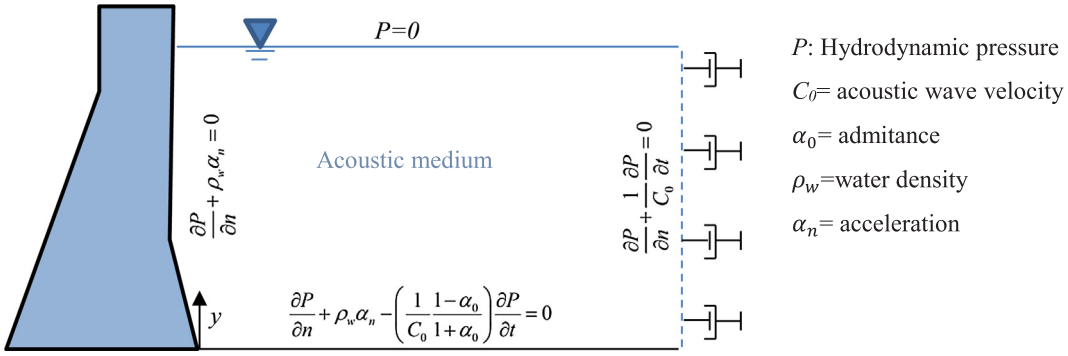

Fig. 1. Dam-reservoir-foundation system and boundary conditions.

reservoir and *y* the vertical coordinate at the upstream face of the dam wall. This technique implies that the hydrodynamic pressures of the water on the dam upstream face during an earthquake are the same as that when a certain body of water moves back and forth with the dam while the remainder of the reservoir is left inactive. This equation is implemented in an Abaqus user subroutine that adds the mass from water to the upstream dam face. Infinite elements are used for far-field rock boundaries; seismic waves are not allowed to reflect into the rock field when they pass across the boundaries of the rock domain.

2.5. Numerical implementation

ASR is a long term process and often continues for many years. As a result, a suitable time step size must be selected to insure sufficient accuracy of results and optimised computational time. The starting point of the analysis of the sequentially coupled problem of heat-diffusion and chemo-mechanical model is the solving of transient thermal analysis with initial boundary conditions. Then, the mechanical structural analysis is performed. This requires a number of parameters, among them:

- The air temperature variations;
- The spatial and temporal variation of the water temperature;
- The concrete thermal properties and
- Mechanical properties of the concrete and damage-plasticity parameters such as the E-Modulus and Poisson's ratio, compressive and tensile nonlinear stress-strain/COD curves and damage variables in tension and compression.

For thermal analysis, and the subsequent mechanical analysis, an appropriate analysis time increment, must be defined. The implementation flowchart of the ASR model which is coupled with the CDP constitutive modelling of concrete illustrated in Fig. 2. This figure shows the relationships between variables in the SU-ASR code (Stellenbosch University ASR FE-code) and explains the code input and output variables incorporated in the code. The current code is implemented in an implicit framework in which Newtown's method as a numerical technique for solving nonlinear equations is used. Because, a non-associated plastic flow rule is used to develop the plastic strains, a non-symmetric numerical solver needs to be used in the finite element modelling of concrete structures using the SU-ASR code.

3. Numerical analysis of Fontana dam affected by ASR

The Fontana dam, a 147 m high concrete gravity dam, with a 720 m crest length and a base thickness of 114 m, was completed in 1944 in the Tennessee River in North Carolina, USA. In 1948, a pattern of map cracking together with upstream movements were observed in the parapets and continued extending over a number of years. Inspection in 1972 due to increasing concerns, led to discovery of cracking inside the foundation gallery near the left flank [17].

The chemo-thermo-damage-plastic model is used to simulate and interpret this phenomenon in the Fontana dam. The cracked section is analysed using the proposed numerical model, to evaluate the pattern of damage generated by mechanical loads and ASR. Sloan and Abraham [29] investigated three gravity blocks of the Fontana dam. One of the main blocks that suffered from severe ASR is Block 35 with 36 m height (see Fig. 3). The crack observed during the inspection is mainly located in this block. In the thermal analysis, the downstream filled-soil and the rock foundation are considered, as they have different conductivity and thermal-diffusion properties than concrete. See Table 1. For the mechanical analysis, about 4500 4-node, quadrilateral, plain strain elements of Abaqus type CPE4R are used with reduced integration. Service loading namely gravity, seasonal temperature variations and hydrostatic pressure are applied. For simplicity, only the dam structure is modelled in the mechanical analysis, with a fixed boundary condition along the dam foundation. A preliminary heat diffusion analysis is performed including the downstream soil fill, rock foundation and concrete domains. Seasonal temperature variations for the upstream and downstream surfaces of the dam are incorporated in the transient thermal analysis are shown in Fig. 4. The initial temperature field is shown in Fig. 5 and is obtained using an average temperature for the upstream, downstream, soil fill material and foundation boundary surface areas.

Fig. 6 illustrates the ASR kinetics and tensile damage at instants during 10 years. At the beginning, the temperature increases through a thin layer from downstream and gradually diffuses to the dam body. Gravity, hydrostatics loads, as well as the boundary constraints increase the compressive stresses along a narrow band which gradually moves into the dam body. When kinetics of the reaction at this band reaches the asymptotic value, strains exceed the tensile strength of the concrete around the gallery due to the strain compatibility condition and therefore cracks will be opened. These findings are in good agreement with observed cracks inside the gallery as shown in Fig. 6b. The ASR progresses further, and after 8 years, another crack zone appears in the lower-right side of the gallery and initially propagates at a similar slope as the first cracks, but soon after turns toward the rock foundation upstream of the dam (see Fig. 6f). It is worth noting that mathematically, this crack will remain stable during the subsequent phases of the analysis. This mechanism is likely due to the fact that the upstream side of the dam is not exposed to a high temperature gradient and kinetics of the ASR is not activated during these years. As can be seen in Fig. 6h, the model predicts initiation of another crack in the downstream face of the dam. This crack propagates toward the internal gallery and finally intersects with the older crack. One can conclude that after 8 years, the ASR extent reaches the gallery and causes high compressive stresses inside the dam. Irreversible plastic strains and cracks in the downstream face are basically due to strain compatibility with high constrained stresses around the gallery. To evaluate the global behaviour of the dam structure, it is also important to assess the strain rate and

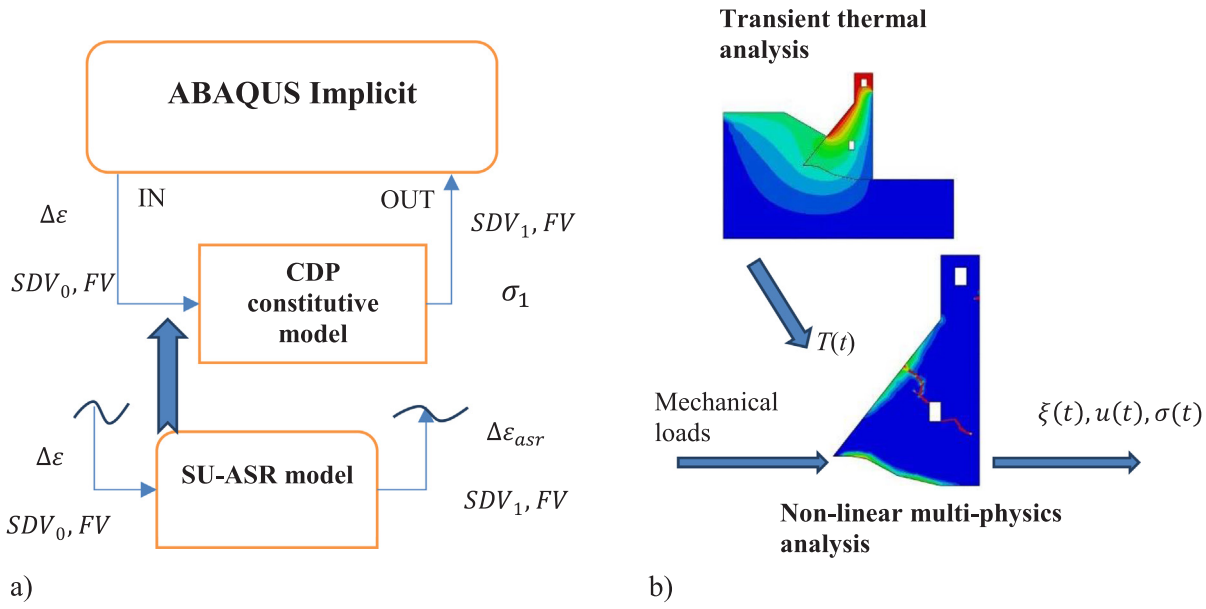

Fig. 2. (a) Numerical framework for the SU-ASR model coupled with CDP constitutive model for concrete material (SDV: Solution Dependent Variable, FV: Field Variable). (b) An example showing the sequential analysis procedure.

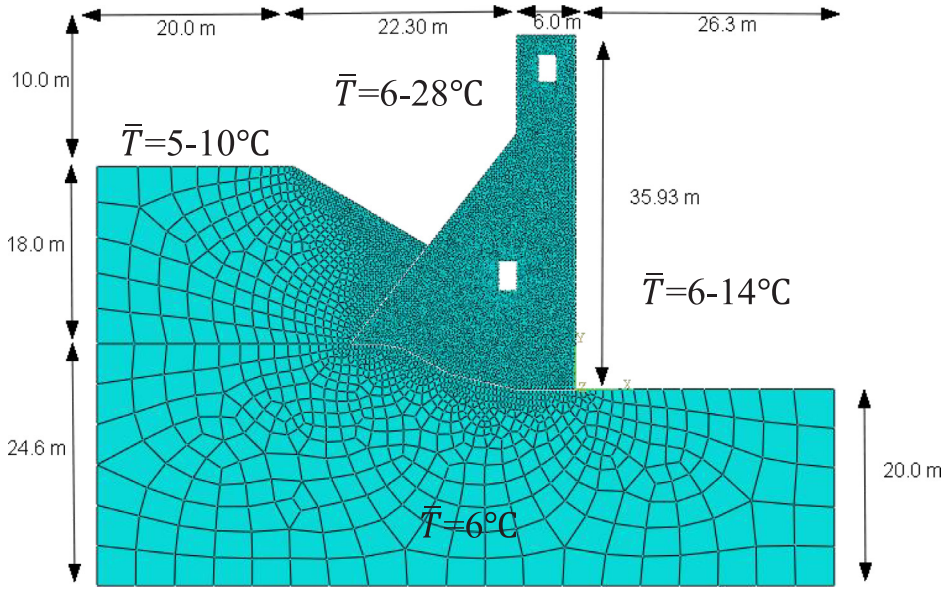

Fig. 3. Geometry and FE model of Fontana dam and mean temperature values, showing the section through Block 35 of the dam wall. Temperatures are expressed in °C, but transformed to Kelvin in computations.

Table 1
Material properties of the Fontana dam structure, foundation and filled soil.

	Young modulus E_0 (GPa)	Poisson's ratio ν	Tensile strength f_t (MPa)	Fracture energy G_t (N/m)	Thermal conductivity k (W/(m K))	Specific heat c (KJ/(kg K))	Thermal expansion coefficient α (10^{-5})
Concrete	22.0	0.17	2.1	200.0	1.75	0.75	1.0
Rock	20.0	0.25	–	–	0.75	0.85	0.5
Filled soil	0.15	0.2	–	–	0.55	1.00	0.5

displacements of the dam at the crest level [30]. Figs. 7 and 8 illustrate the strain rate, horizontal and vertical displacements. From these figures it is observed that the dam crest has experienced a constant crest displacement rate in the downstream direction of about 4.5 mm/year.

4. Combined action of ASR and dynamic excitation

The Koyna dam, completed in 1964 in the region of Maharashtra (India), developed cracks on one of the non-overflow monoliths in a devastating earthquake of magnitude 6.5 M_w on 11 December 1967 [20]. See Figs. 9 and 10. The proposed model is used to predict the long term behaviour of the dam due to a synthetic ASR, and then the current

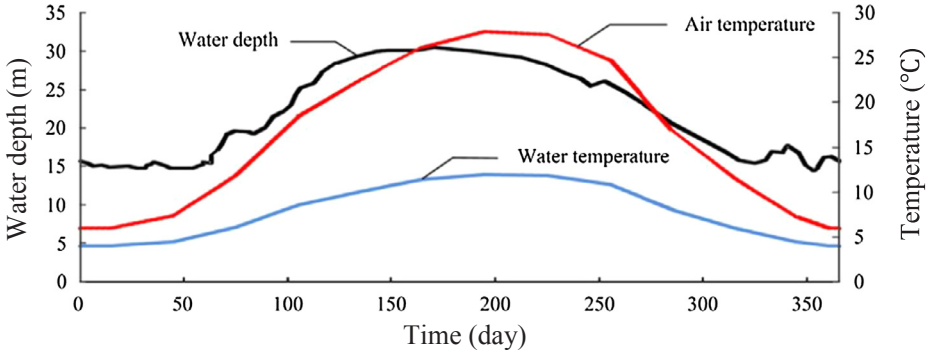

Fig. 4. Seasonal variation of air and water temperature for performing the transient thermal analysis.

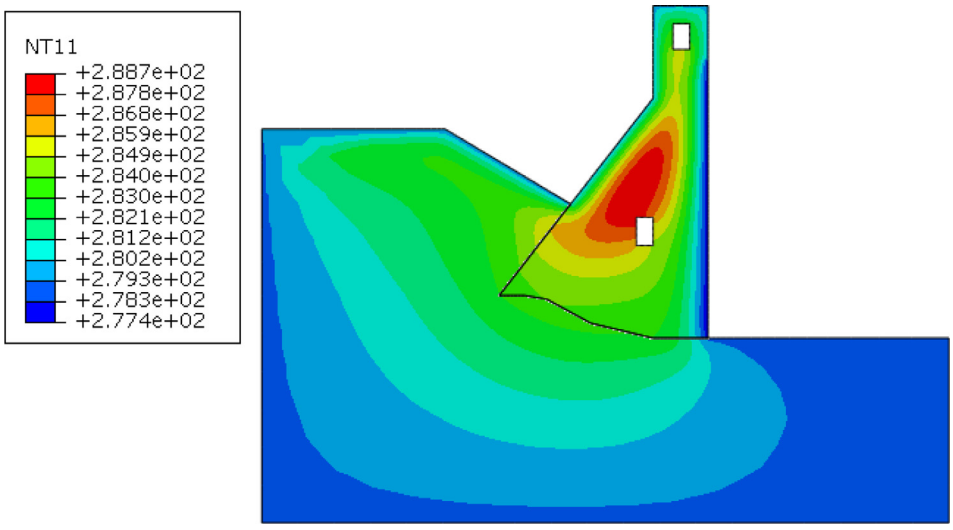

Fig. 5. Computed initial temperature field in Kelvin for the Fontana dam. This temperature is used as an initial condition for transient thermal analysis.

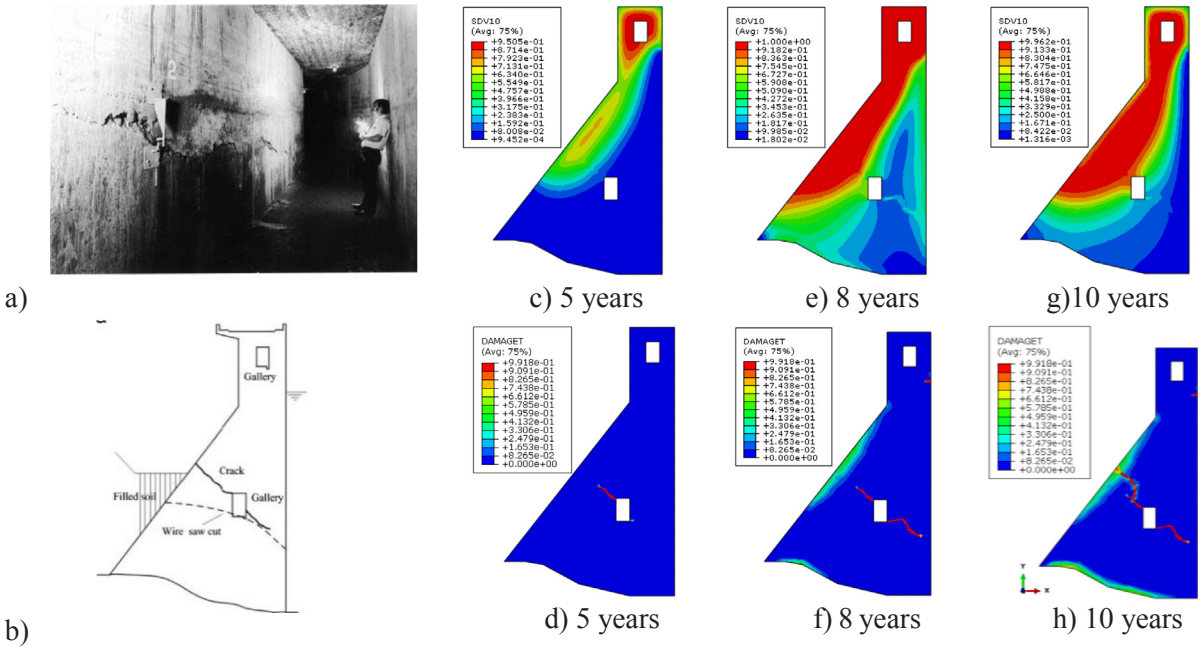

Fig. 6. Reaction extent and tensile damage variation for a period of 10 years for Block 35.

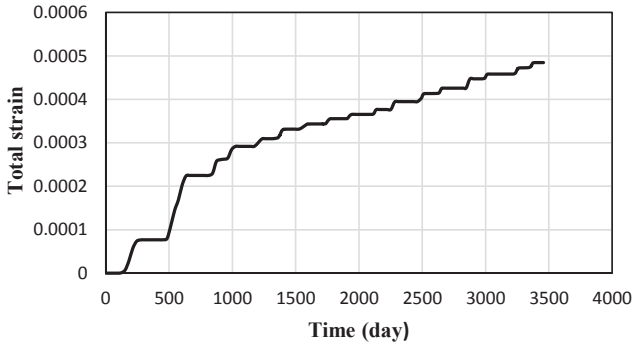

Fig. 7. Horizontal strain vs. time at crest.

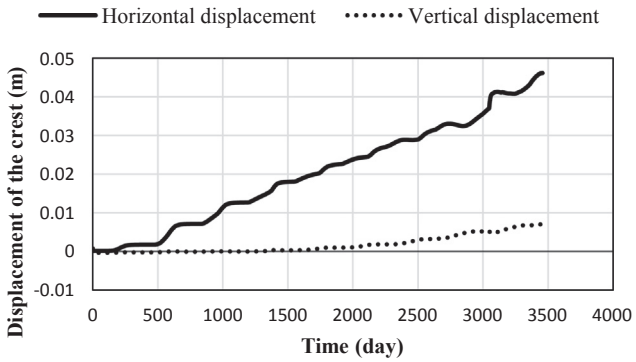

Fig. 8. Vertical and horizontal displacement vs. time at the crest level.

state of the structure is used as an initial state for the seismic analysis. The response of the dam is validated by analysing the Koyna dam under seismic loads with three different assumptions, empty reservoir, added-mass technique and FFSI and comparing the results with experimental research performed on this dam. Then, combined action of ASR and seismic loads is studied to evaluate the long-term behaviour.

4.1. ASR modelling of Koyna dam

The Koyna dam geometry is shown in Fig. 9. The material properties of the dam in the present study are: modulus of elasticity of the dam, E_0 = 31,500 MPa; Poisson's ratio = 0.20 and mass density = 2643 kg/m^3 [9]. ASR damage is defined as a field variable in the code that shows the material deterioration during the service life of the structure in terms of E modulus and tensile strength. Non-uniform degradation of concrete material is considered. ASR kinetics parameters are assumed to be $\tau_l = 200$ days, $\tau_c = 80$ days and $\beta = 0.3\%$. The upstream and downstream average temperatures are assumed as: $T = 5\,^{\circ}$C and $T = 25\,^{\circ}$C, respectively. Fig. 11 shows the result of the ASR analysis of Koyna dam. The extent of the reaction, ASR damage and tensile damage contours are plotted after 10 years. It is observed that the dam experiences a tensile damage mainly in the downstream face due to exposure to the larger thermal gradient. Fig. 11b shows the non-uniform material degradation that are used for the subsequent seismic analysis as an initial state. Fig. 12 shows the crest displacement versus time for the Koyna dam including the gravity and hydrostatic loads without considering the seismic excitation. The maximum displacement after 10 years is −195.5 mm in horizontal direction which implies an average rate of 19.55 mm/year.

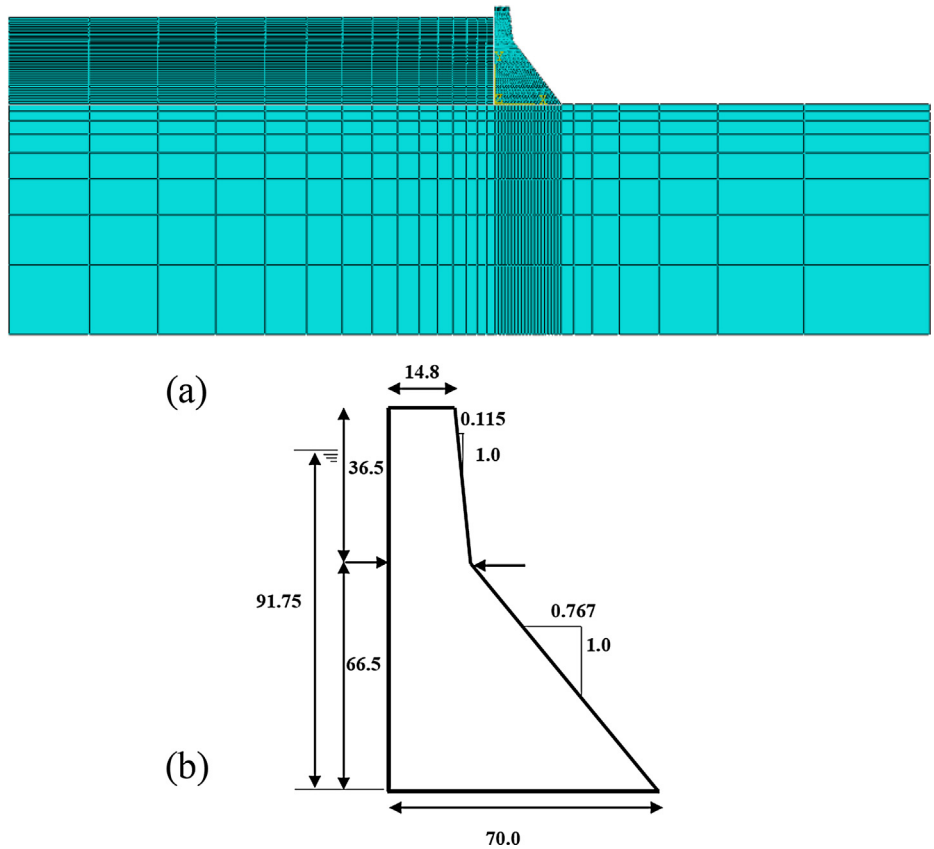

Fig. 9. Numerical model and the geometry of the Koyna dam, (a) finite element mesh of the Koyna dam-water-foundation system and (b) geometry of the dam [9] (units are in meter).

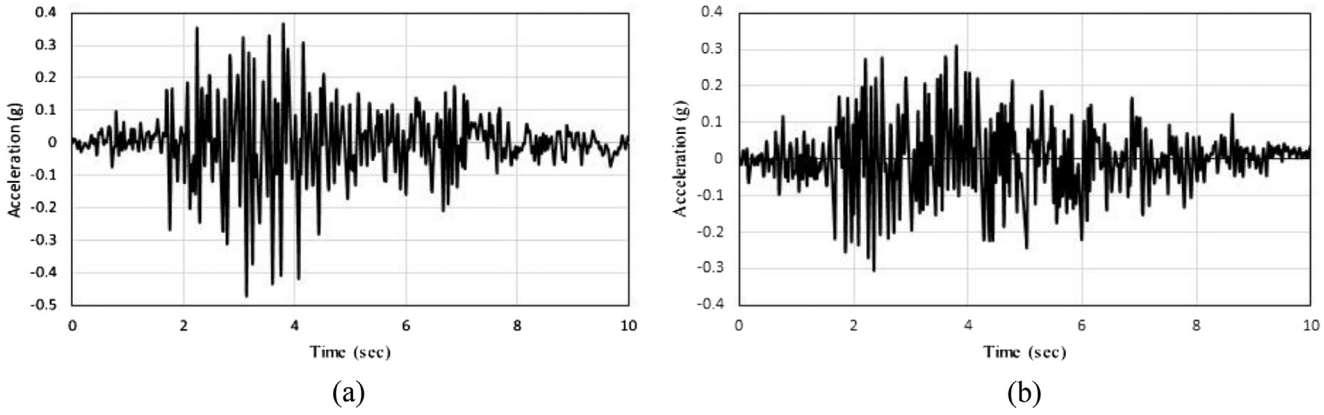

Fig. 10. (a) Horizontal and (b) vertical earthquake acceleration histories for the Koyna dam [9].

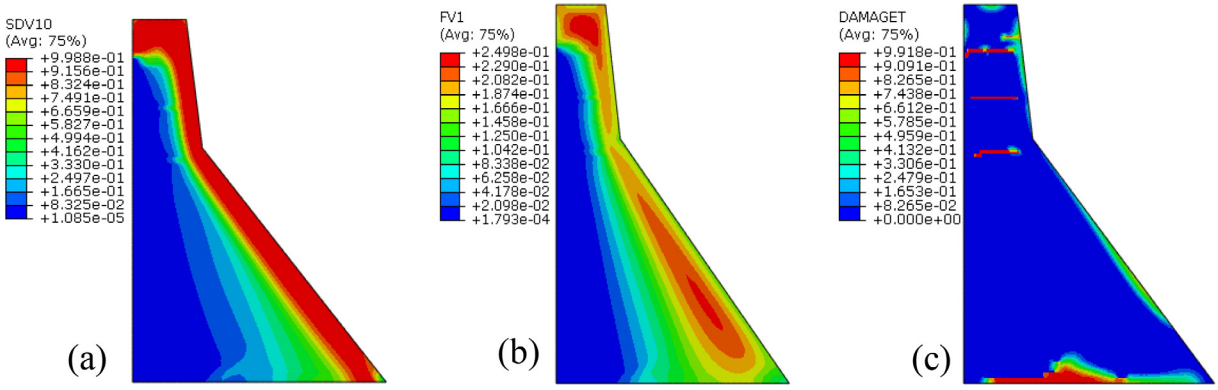

Fig. 11. Koyna dam (a) reaction extent, (b) ASR damage and (c) tensile damage after 10 years.

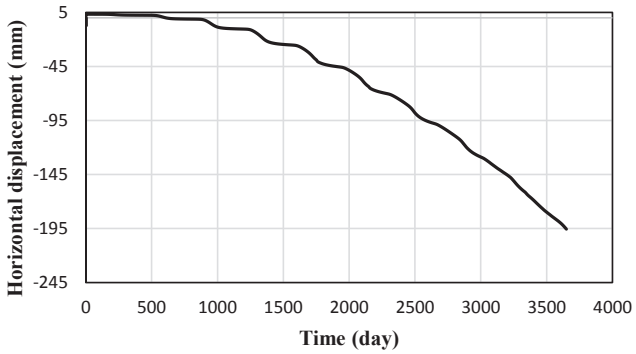

Fig. 12. Horizontal displacement at crest of Koyna dam for 10 years affected by ASR.

4.2. Combined action of ASR and seismic load

From forced vibration tests on dams [31], damping ratios in the range 2–5% have been determined. In implicit dynamic analysis, dissipation mechanisms such as dashpot model components or inelastic material behaviour can be applied. In this study damping ratio used is $\zeta_1 = 3\%$ fraction of critical damping for the first mode of vibration of the dam. From a natural frequency extraction analysis, the first mode of vibration of the dam is found to be $\omega_1 = 18.61$ rad/sec. By assuming Rayleigh stiffness-proportional damping, $\eta = \frac{2\zeta_1}{\omega_1}$ is computed to be $\eta = 3.23 \times 10^{-3}$ sec. The acoustic wave velocity of water, C_o, used is 1438.5 m/s. The loading consists of self-weight of the dam, hydrostatic and hydrodynamic effects of the reservoir and the transverse and vertical components of earthquake loading. The hydrodynamic loading is modelled by applying two assumptions of the reservoir modelling: incompressible fluid using added-mass technique and compressible, inviscid, small amplitude motion, irrotational fluid with the Helmholtz equation and appropriate boundary conditions as mentioned in the previous section [28]. The dam is analysed in the time domain using Newton's method as a numerical technique for solving non-symmetrical nonlinear equilibrium equations using a time step of 0.02 s. The numerical analyses are carried out for two cases, without ASR, and with ASR deterioration for 10 years. Before analysing the dam for combined action of synthetic ASR and actual seismic load, the seismic response of the dam model is validated for three different reservoir modelling strategies of (a) empty reservoir; (b) added mass technique; (c) FFSI with compressible fluid. Structural responses and damage parameters are obtained for both cases to evaluate the seismic performance of the dam considering effects from ASR. Fig. 13 shows the result of the analysis for the Koyna dam without the ASR for (a) empty reservoir; (b) added mass technique and (c) FFSI modelling. The results for added-mass technique and FFSI are in good agreement with experimental modelling. Fig. 14 illustrates the comparison of tensile damage for the both experiment and numerical model at the end of the seismic loading. It is observed that the computed crack pattern is in reasonable agreement with the crack pattern in the experiment. The result of the combined analysis of the ASR and seismic load for tensile damage is shown in Fig. 15. This figure shows that severe damage in the body of the dam mainly due to reduction in stiffness has occurred. The dam experiences several localised cracks in the downstream parapet wall which these cracks propagate mainly through the interior body of the structure and change the dynamic behaviour of the dam. The thermal gradient is at a maximum on the downstream surface of the dam wall which leads to the higher ASR strains in comparison to the upstream wall surface, where the temperature is lower due to the contact of this surface with water in the reservoir.

Furthermore, Figs. 16 and 17 show the time histories of horizontal

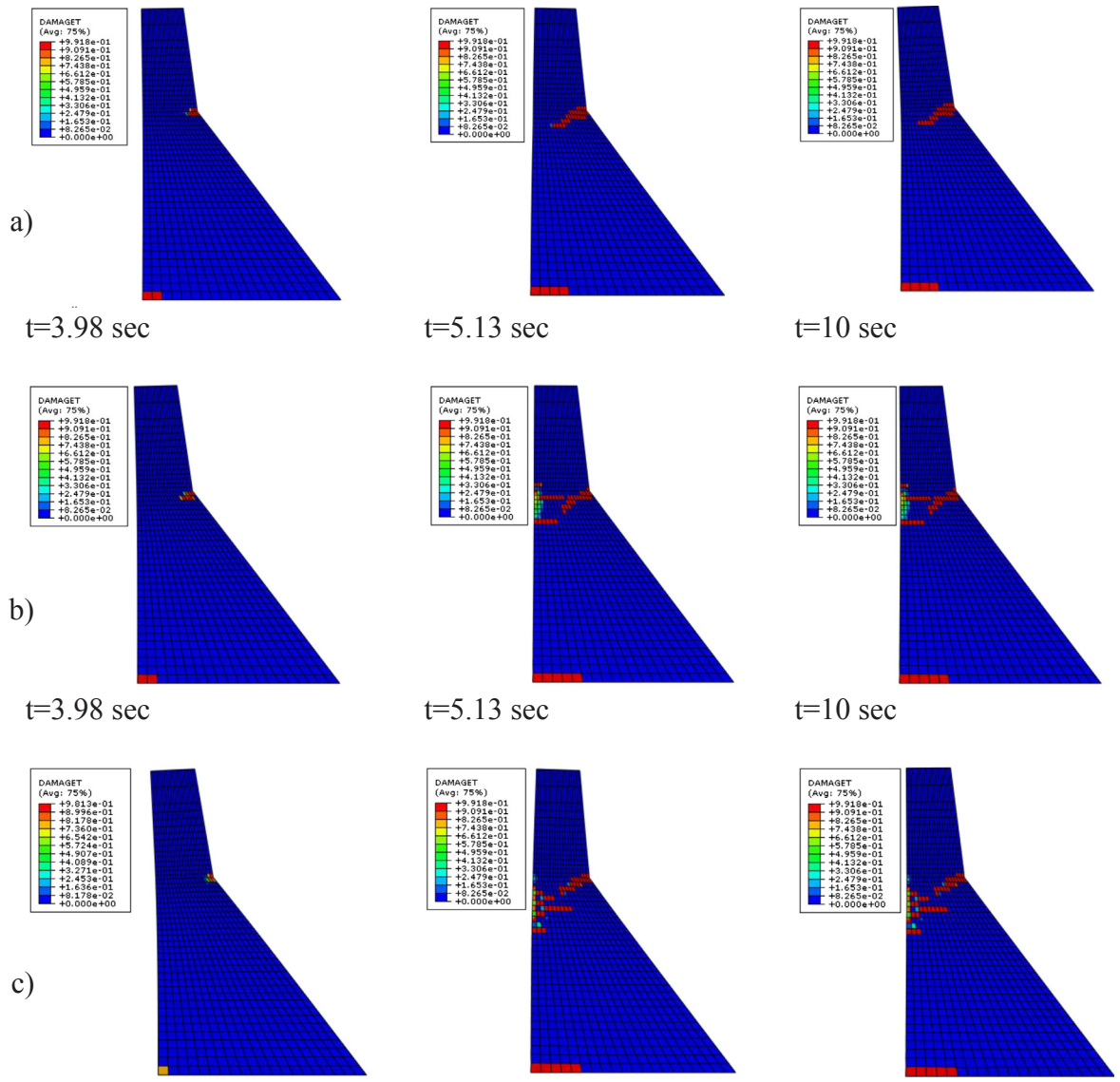

Fig. 13. Results of Koyna dam due to seismic loading at given times and without ASR. The contours show tensile damage variable in the dam wall (a) empty reservoir, (b) added mass technique and (c) FFSI modelling.

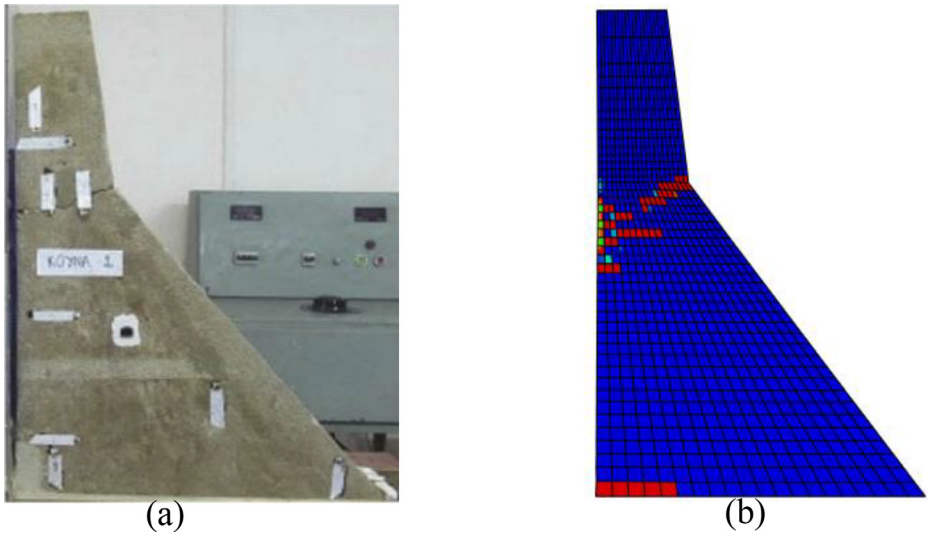

Fig. 14. (a) Experimental [18] and (b) numerical modelling of Koyna dam due to earthquake.

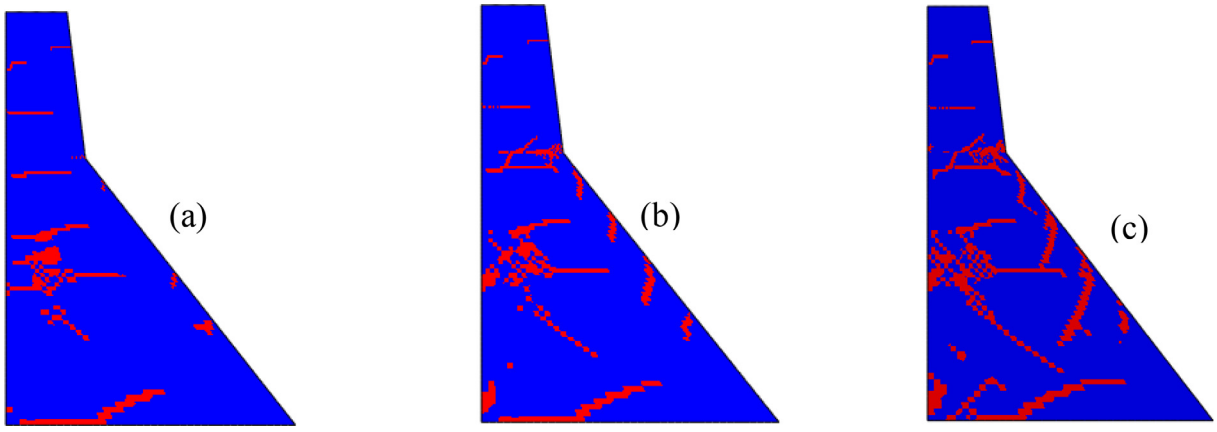

Fig. 15. Contours showing the tensile damage of combined action of ASR and seismic analysis of the Koyna dam using the FFSI strategy to model the reservoir, (a) after 5 sec, (b) after 7 sec and (c) after 10 sec, (note that this analysis is done after 10 years of ASR induced degradation in the dam).

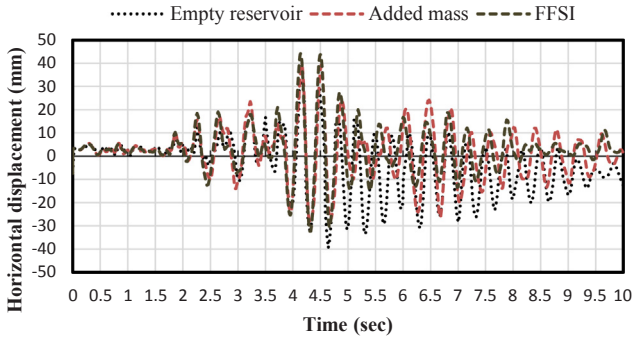

Fig. 16. Comparison of crest horizontal displacement of non-affected ASR dam.

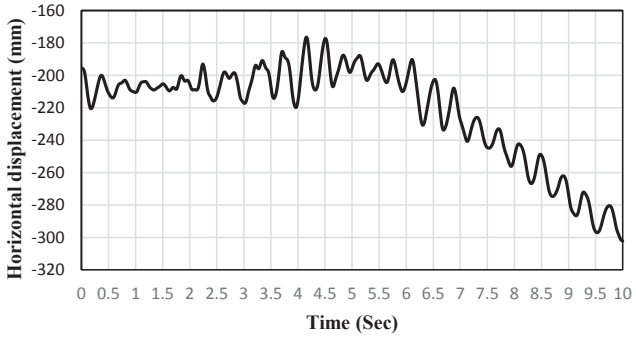

Fig. 17. Horizontal displacement for combined action.

displacement at the dam crest for modelling without ASR and combined action of ASR and seismic load, respectively. The displacement of the ASR affected dam is larger than the case when ASR is not considered. This is due to the decrease in the material stiffness of the concrete and inelastic behaviour and damage in the dam with crack opening. The maximum crest displacement for the combined action of ASR and seismic load for FFSI modelling strategy is 302.2 mm, which is significantly larger than the crest displacement when only ASR effect is considered and is equal to 195.5 mm (see Fig. 12). It is worth noting that due to the combined action of seismic load and ASR an irreversible horizontal displacement of 106.7 mm is added to the dam horizontal displacement when only ASR effect is considered.

5. Conclusion

In this research, the SU-ASR FE-code model is developed and implemented as a user subroutine in Abaqus, a commercial finite element code. In this model, the heat-diffusion analysis is decoupled from the mechanical analysis, and the output from preliminary thermal analysis is used as a predefined field for the subsequent analysis including ASR and mechanical damage. In this chemo-thermo-mechanical FE model, ASR kinetics is combined with damage plasticity model using a finite element approach, which takes the ASR expansion with the effects of temperature, confinement from 3D stress state and time dependent material degradation, into account. The following conclusions are drawn:

- In applying the model to the Fontana gravity dam to predict the long-term behaviour of the dam due to ASR deterioration, the crack patterns and displacements are simulated in good agreement with the field observations.
- Seismic response of the Koyna dam, after it developed a damaged state through ASR deterioration, is captured in good agreement with experimental findings. Three assumptions are used for modelling the water-dam interaction mainly as empty reservoir, added-mass technique and FFSI with Helmholtz wave equation. The FFSI modelling strategy predicts the damage pattern better than the other approaches by comparing the crack pattern and crest displacement.
- There is a difference in displacement response of an ASR-affected and non-affected concrete dam indicating that the vibration characteristic of the dam is significantly changed due to crack opening and non-uniform material degradation caused by ASR. The seismic displacement response of the ASR affected dam is larger than that of the non-affected dam. During the earthquake cracks propagate through the upper face of the dam which may cause collapse of the dam.

In this research, long term strains such as creep, relaxation and shrinkage are not considered and future research and modelling should be conducted to include these phenomena. Whilst computational procedures exist to incorporate these time-dependent phenomena, appropriate model parameter characterisation remains a challenge given the level of measured data for particular structures. Also, FE modelling of a rehabilitated dam to assess the effectiveness of the remedial actions is another topic for the future research. Although extensive research has been done to model ASR and other internal swelling reactions in concrete structures, limited attention has been paid to develop an engineering solution to solve these problems for real life dams exposed to these problems. It is foreseen that this research could stimulate research activity by other researchers and engineers active in this field to further develop and extend the models of the different mechanisms involved in these deleterious phenomena, presented here.

Acknowledgements

The research is funded by The Concrete Institute (TCI) and the Department of Trade and Industry of South Africa under THRIP Research Grant TP14062772324.

Appendix A. Supplementary material

Supplementary data to this article can be found online at https://doi.org/10.1016/j.engstruct.2019.05.087.

References

[1] Bažant ZP, Steffens A. Mathematical model for kinetics of alkali-silica reaction in concrete. Cem Concr Res 2000;30:419–28.
[2] Ulm F, Coussy O, Kefei L, Larive C. Thermo-chemo-mechanics of ASR expansion in concrete structures. J Eng Mech 2000;126(3).
[3] Saouma VE, Martin RA, Hariri-Ardebili MA, Katayama T. A mathematical model for the kinetics of the alkali-silica chemical reaction. Cem Concr Res 2015;68:184–95.
[4] Larive C. Apports Combin'es de l'Experimentation et de la Modélisation à la Comprehension del'Alcali-Réaction et de ses Effets Mécaniques. PhD thesis. Paris; 1998.
[5] Multon S, Toutlemonde F. Effect of applied stresses on alkali–silica reaction-induced expansions. Cem Concr Res 2006;36(9):12–20.
[6] Aluad S Mohamad. Durability of concrete under combined action: Mechanical load and ASR PhD thesis SA: Stellenbosch University; 2016
[7] Giorla AB, Scrivener KL, Dunant CF. Influence of visco-elasticity on the stress development induced by alkali–silica reaction. Cem Concr Res 2015;70.
[8] Tan H, Chopra AK. Earthquake analysis of arch dams including dam-water-foundation rock interaction. Earthq Eng Struct Dyn 1995;24:1453–74.
[9] Calayir Y, Karaton M. Seismic fracture analysis of concrete gravity dams including dam-reservoir interaction. Comput Struct 2005;83(19–20):1595–606.
[10] Charlwood RG, Solymar SV, Curtis DD. A review of alkali aggregate reactions in hydroelectric plants and dams. Proceedings of the international conference of alkali-aggregate reaction in hydroelectric plants and dams, Fed., Canada 1992;129.
[11] Capra B, Sellier A. Orthotropic modelling of alkali-aggregate reaction in concrete structures. Num Sim Mech Mater 2003;35:817–30.
[12] Saouma V, Perotti L. Constitutive model for alkali aggregate reactions. ACI Mater J 2006;103.
[13] Dormieux L, Kondo D, F.J., Ulm,. Microporo mechanics. England: John Wiley & Sons Ltd.; 2006.
[14] Dunant C, Scrivener K. Micro-mechanical modelling of alkali-silica reaction-induced degradation using the AMIE framework. Cem Concr Res 2010;40:517–25.
[15] Comby-Peyrot I, Bernard F, Bouchard P, Bay F, Garcia-Diaz E. Development and validation of a 3d computational tool to describe concrete behaviour at mesoscale. Application to the alkali-silica reaction. Comput Mater Sci 2009;46(4):1163–77.
[16] Esposito R, Hendriks MAN. Literature review of modelling approaches in concrete: a new perspective. Eur J Environ Civ Eng 2017. https://doi.org/10.1080/19648189.2017.1347068.
[17] Ingraffea AR. Case studies of simulation of fracture in concrete dams. Eng Fract Mech 1990;35.
[18] Comi C, Fedele R, Perego U. A chemo-thermo-damage model for the analysis of concrete dams affected by alkali-silica reaction. Mech Mater 2009;41:210–30.
[19] Valliappan S, Chee C. Ageing degradation of concrete dams based on damage mechanics concepts. In: Yuan Y, Cui J, Mang H, editors. Computational structural engineering. Netherlands: Springer; 2009. p. 21–35.
[20] Mridtha S, Maity D. Experimental investigation on nonlinear dynamic response of concrete gravity dam-reservoir system. Eng Struct 2014;80:289–97.
[21] Lee J, Fenves LG. Plastic damage model for cyclic loading of concrete structures. J Eng Mech ASCE 1998;124.
[22] Simulia. Abaqus 2016 theory guide. Dassault Systemes; 2016.
[23] Bažant Z, Oh BH. Crack band theory for fracture of concrete. Mater Struct 1983;16:155–77.
[24] Pan J, Xu Y, Jin F, Zhang C. A unified approach for long term behaviour and seismic response of AAR-affected concrete dams. Soil Dyn Earth Eng 2014;63:193–202.
[25] Liaudat J, Carol I, Lopez C, Saouma V. ASR expansion in concrete under triaxial confinement. Cem Concr Com 86 2018.
[26] Govevski V, Yildiz E. Numerical analysis of AAR affected structures with slot-cuts DSC. Wiley ISTE; 2017.
[27] Inst. of Struc. Eng., Structural effects of alkali-silica reaction, Technical guidance on the appraisal of existing structures. Technical report. Report of an ISE task group; 1992.
[28] Zienkiewicz OC, Taylor RL, Zhu J. The finite element method for solid and structural mechanics. 6th ed. Elsevier Butterworth Heinemann; 2005.
[29] Sloan RC, Abraham TJ. TVA cuts deep slot in dam ends cracking problems. Civ Eng 1978;48.
[30] Sellier A, Grimmal E, Multon S, Bourfarot E. Swelling concrete in dams and hydraulics structures. SDC: Wiley; 2017.
[31] Chopra AK. Dynamics of structures. 4th ed. Pearson; 2012.